PLOS ONE

RESEARCH ARTICLE

The expression of equine keratins K42 and K124 is restricted to the hoof epidermal lamellae of *Equus caballus*

Caitlin Armstrong[1], Lynne Cassimeris[2], Claire Da Silva Santos[2], Yagmur Micoogullari[2¤], Bettina Wagner[3], Susanna Babasyan[3], Samantha Brooks[4], Hannah Galantino-Homer[1]*

1 Department of Clinical Studies, New Bolton Center, University of Pennsylvania, School of Veterinary Medicine, Kennett Square, Pennsylvania, United States of America, 2 Department of Biological Sciences, Lehigh University, Bethlehem, Pennsylvania, United States of America, 3 Department of Population Medicine and Diagnostic Sciences, College of Veterinary Medicine, Cornell University, Ithaca, New York, United States of America, 4 Department of Animal Sciences and University of Florida Genetics institute, University of Florida, Gainesville, Florida, United States of America

¤ Current address: Department of Pathology, Brigham and Women's Hospital and Harvard Medical School, Boston, Massachusetts, United States of America

* hghomer@vet.upenn.edu

Check for updates

🔓 OPEN ACCESS

Abstract

The equine hoof inner epithelium is folded into primary and secondary epidermal lamellae which increase the dermo-epidermal junction surface area of the hoof and can be affected by laminitis, a common disease of equids. Two keratin proteins (K), K42 and K124, are the most abundant keratins in the hoof lamellar tissue of *Equus caballus*. We hypothesize that these keratins are lamellar tissue-specific and could serve as differentiation- and disease-specific markers. Our objective was to characterize the expression of K42 and K124 in equine stratified epithelia and to generate monoclonal antibodies against K42 and K124. By RT-PCR analysis, keratin gene (*KRT*) *KRT42* and *KRT124* expression was present in lamellar tissue, but not cornea, haired skin, or hoof coronet. In situ hybridization studies showed that *KRT124* localized to the suprabasal and, to a lesser extent, basal cells of the lamellae, was absent from haired skin and hoof coronet, and abruptly transitions from *KRT124*-negative coronet to *KRT124*-positive proximal lamellae. A monoclonal antibody generated against full-length recombinant equine K42 detected a lamellar keratin of the appropriate size, but also cross-reacted with other epidermal keratins. Three monoclonal antibodies generated against N- and C-terminal K124 peptides detected a band of the appropriate size in lamellar tissue and did not cross-react with proteins from haired skin, corneal limbus, hoof coronet, tongue, glabrous skin, oral mucosa, or chestnut on immunoblots. K124 localized to lamellar cells by indirect immunofluorescence. This is the first study to demonstrate the localization and expression of a hoof lamellar-specific keratin, K124, and to validate anti-K124 monoclonal antibodies.

Introduction

The skin and its appendages are made of stratified epithelia composed of keratinocytes, defined by expression of keratin intermediate filament proteins (abbreviated K for proteins and *KRT* for genes) [1]. Keratin filaments resist stretching (strain) and provide tensile strength to epithelia and skin appendages. Tissue- and differentiation-specific variation in specific keratin isoform content determines the physical and mechanical properties of diverse epithelial tissues and of their keratinocyte building blocks [2;3]. Understanding how keratins function to provide mechanical stability is crucial to our understanding of human and animal diseases associated with keratin mutations or abnormal keratin expression [4–8]. Here we describe unique keratins of the equine (*Equus caballus*) epidermal lamellae, a highly specialized tissue that withstands extreme force and provides a model for understanding how keratins provide mechanical strength to flexible tissues.

Keratins form obligate heterodimers between specific type I ("acidic," e.g., K42) and type II ("basic to neutral," e.g., K124) keratin isoforms [9]. All keratins have a central α-helical rod domain and globular head (amino-end) and tail (carboxy-end) domains [4;9]. The rod domains intertwine in a coiled-coil fashion to form heterodimers and tetramers which associate to form 10 nm diameter filaments [9]. In the cell, the interactions between keratin filaments and desmosomes and hemidesmosomes integrate and provide mechanical stability to epithelial tissues [10]. Keratin filaments must be cross-linked into bundles of varying diameter to play a significant role in structural support [2;11]. This self-organization into filaments and bundles is mediated, in part, by specific covalent and non-covalent interactions between the head or tail domain of one keratin and rod domains of another keratin and are unique for each keratin isoform pair [2;11]. Amino acid sequence variations in these regions in keratin isoforms therefore directly contribute to the mechanical properties of keratin filaments and cytoskeletal networks and to the diversity of stratified epithelia and epidermal appendages, including the hoof capsule.

Each single-toed foot of a 500 kg horse (*E. caballus*) must withstand peak ground reaction forces of 2–5,000 N while protecting the underlying limb from trauma [12;13]. The equine adaptation to single-toed unguligrade locomotion requires the integration of the musculoskeletal system with a cornified hoof capsule and the strong, but flexible, suspension of the distal phalanx from the inner surface of the hoof capsule [14–16]. As shown in Fig 1, the inner epithelium of the equine hoof capsule, which is homologous to the nail bed [17], is folded into primary and secondary epidermal lamellae (PELs and SELs, respectively). PELs and SELs increase the surface area of epidermal-dermal attachment and, with the dermal connective tissue to which it adheres, form the suspensory apparatus of the distal phalanx (SADP) [15]. Laminitis, a common and crippling foot disease of equids and other ungulates, is associated with microanatomical and molecular lesions of the epidermal and dermal lamellae that can progress to structural failure of the SADP and dysplastic changes in the hoof and underlying tissues [15;18–20]. In spite of the importance of the hoof lamellae for equine locomotion and disease, few aspects of hoof lamellar biology, including keratin isoform composition, have been well characterized.

Equine keratin isoform expression and localization has relied entirely on commercial antibodies, many of which cross-react with multiple keratin isoforms [21;22]. Similar to other stratified epithelia, hoof lamellae express K14 in the basal cell layer and also express unique keratin isoforms that contribute to the health and disease of this tissue [23;24]. By proteomics, we discovered two novel equine keratins, K42 and K124 [23]. These keratins are the most abundant cytoskeletal proteins in equine hoof lamellae, accounting for over 50% of the total keratin content of this tissue [23].
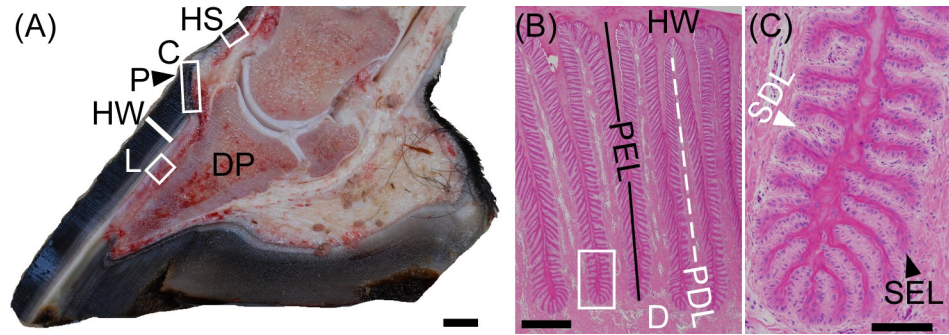
Fig 1. Macroscopic anatomy of the equine (*E. caballus*) foot and microscopic anatomy of the hoof lamellae. (A) Equine foot, midsagittal section, showing locations of samples retrieved for this study: HS: haired skin and the following hoof capsule regions: C: coronet (proximal stratum medium layer and nail matrix homolog), P: periople (stratum externum layer and cuticle homolog), HW: hoof wall (stratum medium layer and nail plate homolog), L: lamellar tissue, including epidermal lamellae (stratum internum layer and nail bed homolog), dermal lamellae, and dermal corium up to the surface of the distal phalanx (DP). Scale bar: 1 cm **(B)** Transverse section of the lamellar region (H&E stain). HW, at the top of the image, is contiguous with the approximately 500 cornifying primary epidermal lamellae (PELs) of each hoof capsule which interdigitate with primary dermal lamellae (PDLs). PDLs are in turn continuous with the dermal corium (D), transferring the weight of the horse from the DP to the HW. Scale bar: 500 μm. **(C)** Higher magnification of boxed area in (B). Each PEL has 100–150 secondary epidermal lamellae (SELs; black arrowhead) which interdigitate with secondary dermal lamellae (SDLs).Scale bar: 100 μm.

KRT42 and *KRT124* exist only as pseudogenes in humans, *KRT42P* and *KRT90P*, respectively (the latter was formerly named *KRT124P* when equine *KRT124* was named [1;23;25]). Murine *Krt42* (formerly *K17n* or *Ka22*) mRNA is expressed in the nail unit [26]. A putative *KRT124* ortholog, *Krt90* (formerly *Kb15*), is translated from cDNA libraries in mice and rats [27] and was identified from the draft genomic sequence of the opossum [28]. *KRT42* and *KRT124* were recently identified and mapped to the canine and equine genomes, but their patterns of expression have not been described beyond their identification from RNA-seq data derived from skin biopsies from three dogs and one horse [25]. The lack of isoform-specific antibodies has impeded the detailed investigation of equine hoof capsule or lamellar tissue-specific keratins [24] and mammalian nail unit keratins in other species [17]. The objectives of this study were to characterize the pattern of expression of K42 and K124 in equine stratified epithelia of the hoof and skin and to determine if the most abundant keratins of the hoof lamellae are specific differentiation markers of this highly specialized epithelium. We report here that K42 and K124 expression is restricted to equine hoof lamellae and we have characterized monoclonal antibodies against K124.

Methods

Ethics statement

The protocols, titled 'Pathophysiology of Equine Laminitis (By-products only)' and 'Equine Laminitis Tissue Bank,' under which the archived equine tissue samples used for this study were collected, were approved by the University of Pennsylvania Institutional Animal Care and Use Committee (protocol #801950 and #804262, respectively). Euthanasia of the horses was carried out in accordance with the recommendations in the Guide for the Care and Use of Agricultural Animals in Research in Teaching Federation for Animal Science Societies) and the AVMA Guidelines for the Euthanasia of Animals (American Veterinary Medical Association) by overdose with pentobarbital sodium and phenytoin sodium. Mouse immunization, euthanasia by cervical dislocation, and monoclonal antibody production were carried out in accordance with the recommendation in the Guide for the Care and Use of Laboratory

Animals of the National Institute of Health. The protocol titled 'Mouse Monoclonal Antibody Production' was approved by the Institutional Animal Care and Use Committee at Cornell University (protocol #2007–0079).

Subjects and tissue retrieval

All *E. caballus* subjects are part of a laminitis tissue repository and were euthanized for medical reasons unrelated to this study, as previously described [29]. Subjects had no clinical history, macroscopic or microscopic evidence of hoof, dermatological, or corneal diseases in the tissues used [30]. The age, breed, and sex of each subject are listed in S1 Table. For each experiment, at least three samples from at least three different subjects were used, as detailed in S2 Table. The anatomical locations of tissues dissected from the foot, including haired skin, coronet, and hoof lamellae, are illustrated in Fig 1A. The coronet, or coronary region of the hoof, is homologous to the nail matrix [17]. It is the region from which the hoof wall (nail plate) grows and includes epidermal and supporting dermal tissue at the proximal edge of the hoof capsule. The lamellar tissues samples included the innermost layer of the hoof capsule, which is homologous to the nail bed [17] and is comprised of PELs and SELs, the corresponding primary and secondary dermal lamellae, and the adjacent dermal corium. All tissue samples were collected immediately after euthanasia, as described elsewhere [20;29;31]. Briefly, the foot was disarticulated at the metacarpal/metatarsal-phalangeal joint using an autopsy knife and an approximately 2 cm thick midsagittal section of each foot was made with a band saw. The dorsal hoof wall and adjacent tissues were dissected from the underlying middle and distal phalanges using a number 60 autopsy blade (Becton Dickinson, Franklin Lakes, NJ, USA). The resulting strip of hoof wall and tissues were cut into approximately 2 cm long mid-dorsal lamellar, coronary, and haired skin transverse pieces using the autopsy blade and farrier horseshoe puller tool (Diamond™ 12-inch shoe puller, Cooper Tools, Apex, NC, USA). The autopsy blade was then used to dissect the mid-dorsal lamellar and coronary tissues from the bulk of the hoof wall, cutting 1–2 mm into the inner hoof wall, to trim approximately 1 mm from the band sawed sides of the hoof and haired skin tissues, and to dissect 50–100 mg transverse sections from the regions shown in Fig 1A for snap-freezing or fixation. All other tissues were dissected by scalpel immediately post mortem. Tissue samples were immediately either 1) snap frozen in liquid nitrogen and stored in liquid nitrogen until processed for protein or RNA extraction, 2) formalin-fixed/paraffin-embedded (FFPE) until sectioned for in situ hybridization studies, or 3) paraformaldehyde-fixed/sucrose-dehydrated, embedded, frozen, and stored at -80˚C until sectioned for indirect immunofluorescence, as previously described [23;32].

Extraction and amplification of keratin isoform mRNA

Oligonucleotide primers. Oligonucleotide primers for equine keratin isoforms *KRT10A*, *KRT10B*, *KRT14*, *KRT42* and *KRT124* were designed using Primer3 (http://bioinfo.ut.ee/primer3-0.4.0/)[33] and are listed in Table 1. All oligonucleotides were synthesized by Integrated DNA Technologies, Inc. (Coralville, IA, USA). Alternate forward primers were designed to amplify the two *KRT10* genes, *KRT10A* and *KRT10B*, since the equine *KRT10* gene has undergone duplication [25]. For *KRT124*, one set of primers was designed to amplify the 3' exon (*KRT124 3'*), which shows no homology to known keratins, and a second primer set was designed to amplify a region of the predicted transcript that shows some homology to several keratins (*KRT124 Mid*). For all primers, RT-PCR product sequence was confirmed by Sanger sequencing for at least one band from each positive tissue type (S1 File).

RNA extraction. Archived snap-frozen tissue was pulverized using a liquid nitrogen-chilled, ELIMINase-treated (Decon Labs Inc, King of Prussia, PA, USA) stainless steel mortar

Table 1. PCR Primer sequences.

Primer name[a]	Sequence (5'-3')	Genome target (EquCab 2.0)	mRNA length (bp)	Genomic length (bp)	Gene ID[b]
KRT10A F	AAGGCTCCCTTGGTGGAGGT	chr11:21819187–21820546	555	1363	100146924
KRT10A R	GCACCACATTGGCATTATCA				
KRT10B F	GAGGCTCCTTTGGTGGAGGA	chr11:21835224–21836574	540	1348	100053935
*KRT10B*R	GCACCACATTGGCATTATCA				
KRT14 F	CACCGTGGACAATGCTAATG	chr11:21200031–21201000	258	970	100053489
KRT14 R	CTCACCTGGCCTCTCAGGCT				
KRT42 F	GGAGGACTGGTTCTTCAGCA	chr11:21158291–21159359	268	1069	100066586
KRT42 R	CATGTCACAGCGCAGCTC				
KRT124 Mid F	GGAAGTGGGATGATGTCTGG	chr6:69519215–69521326	261	2112	100061458
KRT124 Mid R	CATGGGCTCGATGTTGG				
KRT124 3' F	GTGCAGACTCACTGGGGAAG	chr6:69510070–69511624	214	1552	100061458
KRT124 3' R	TTAGCTCCTATAACTCCTCTTGGT				

[a]Primer names indicate target equine gene name and forward (F) or reverse (R) primer.

[b]Gene ID: Gene identification number, as per the National Center for Biotechnology Information (NCBI) database.

https://doi.org/10.1371/journal.pone.0219234.t001

and pestle (Bio-pulverizer™, BioSpec Products, Bartlesville, OK, USA) prior to total RNA extraction. Next, total RNA was extracted using the RNeasy Fibrous Tissue Mini Kit (Qiagen, Valencia, CA, USA) by a modified version of the manufacturer's instructions, as follows, to allow for complete disruption and homogenization of the highly fibrous lamellar tissue. Pulverized tissue samples were mixed with 300 μl Buffer RLT, 590 μl RNase-free water, and 10 μl proteinase K by gentle vortexing and incubated at 55°C for 10 min. This mixture was then homogenized by repeated (5-10x) aspiration through an 18 g hypodermic needle and syringe and subjected to centrifugation at 10,000 x g for 10 min. The resulting supernatant was then removed and mixed with 0.5 volume of 100% ethanol, added to the provided RNeasy Mini column in 700 μl increments, and subjected to centrifugation 10,000 x g. RNA retained on the RNeasy column was retrieved by adding 350 μl Buffer RW1 and subjecting it to centrifugation for 15 s at 10,000 x g. DNase treatment and subsequent buffer RW1 and RPE steps were then performed according to the manufacturer's instructions, including the optional final centrifuge step. Final RNA elution was done once in a total volume of 50 μl of RNase-free water. Total RNA was quantified using a Nanodrop 2000 spectrophotometer (Thermo Fisher Scientific, Waltham, MA, USA). Quality was confirmed by checking A260/A280 ratios and ensuring they were 2.0±0.1 for all samples tested.

Qualitative RT-PCR. Reverse transcriptase-polymerase chain reaction (RT-PCR) was carried out on an Eppendorf Mastercycler thermocycler (Eppendorf, Hamburg, Germany) in a single step using the Qiagen OneStep RT-PCR Kit (Qiagen), according to the manufacturer's instructions, in a total reaction volume of 25 μl using 100 ng of total RNA. The RT reaction was done at 50°C for 30 min. The PCR cycling conditions which immediately followed were as follows: 95°C activation step (15 min, 1x) followed by 30 cycles of 3-step PCR (94°C denature for 30 sec, 50°C anneal for 30 sec, 72°C extension for 1 min). The *KRT42* product was produced with the same overall method above but with the following modifications: 66°C anneal; 40 PCR cycles; 2 min extension per cycle with a final 10 min extension (also at 72°C) following completion of all 40 PCR cycles. RT-PCR products were subjected to agarose gel electrophoresis, visualized with SYBR Safe™ DNA stain (Thermo Fisher Scientific, Waltham, MA, USA) and imaged on a UV transilluminator with a digital camera and ethidium bromide filter (Canon G10, Tokyo, Japan).

In situ hybridization

Digoxigenin (DIG)-labeled riboprobes that included unique DNA sequences encoding *KRT14* and *KRT124* were produced by gene synthesis. For *KRT14*, a 297 bp region at the 3' end of the mRNA sequence (NM_001346198; bp 1371–1667) was synthesized. To facilitate cloning, 5' NotI and 3' KpnI restriction sites were included in the synthesized DNA fragment. For *KRT124*, a specific sequence of 684 bp was synthesized that included the 3' end of the coding sequence and a portion of the 3' UTR (XM_001504397.3; bp 1623–2307). 5' NotI and 3' XhoI restriction sites were included in the DNA synthesis. The synthesized DNAs were cloned into pBluescript SK (+) vectors at the multi-cloning site, which includes T7 and T3 RNA polymerase promoter sequences. Plasmid construction was verified by Sanger sequencing (S2 and S3 Files). All gene synthesis, cloning and verification of sequences were performed by Genscript (genscript.com). Digoxigenin (DIG)-labeled riboprobes were synthesized from T7 (for antisense probe synthesis) and T3 (for sense probe synthesis) promoters using MEGAscript Transcription kits (Ambion, Thermo Fisher Scientific) according to the manufacturer's protocol.

In situ hybridization was performed as described, using standard methods [34]. Briefly, FFPE tissue sections were deparaffinized for 2x10 min in xylene, followed by rehydration in a graded ethanol series (100%, 75%, 50% and 25%, 3 min each) and digested for 5 min with proteinase K (10μg/mL; Ambion). Tissue sections were allowed to hybridize overnight in a humid chamber at 65°C with 1 ng/**μ**L of sense (negative probe) or antisense (positive probe) DIG-labeled riboprobes in hybridization buffer containing 50% formamide. After washes in saline-sodium citrate buffer, the sections were incubated with alkaline phosphatase-conjugate anti-DIG Fab fragments (#11093274910, 1:5000, SigmaAldrich, St. Louis, MO, USA) in a humid chamber overnight at 4°C. After washing in PTB (Phosphate Buffered Saline + 0.2% Triton x-100 + 0.1% BSA), labeled probe was visualized using NBT/BCIP substrate (Roche Diagnostics, Indianapolis, IN, USA) resulting in a blue/purple precipitate. PTw buffer (Phosphate Buffered Saline + 0.1% Tween) was used to stop the reaction. Sections were mounted in 80% glycerol/PTw. Images were collected on a Nikon Nti microscope using a Nikon DS /Ti2 color camera and Nikon Elements software (Nikon Instruments, Inc., Melville, NY, USA). Typically images were collected at 10X (brightfield) or at 20X (DIC optics).

Monoclonal antibodies

K42 monoclonal antibody. The entire coding sequence of *KRT42* (gene ID: 100066586) was amplified using gene-specific primers and the total RNA, RT-PCR, and agarose gel electrophoresis methods described in the extraction and amplification of keratin isoform mRNA section. These primer sequences were as follows: ATGGCTGCCACCACCACCAC (forward primer) and GCGATGGCTGCCCCTTGA (reverse primer). The corresponding genomic location is chr11 + 21153825–21160809 (EquCab2.0). Following excision of the band from the agarose gel, K42 was expressed as a fusion protein with equine IL-4 as previously described [35]. In brief, the 1416-bp product was sub-cloned into the mammalian expression vector (pcDNA3.1 (−)/Myc-His, version B, Invitrogen,Carlsbad, CA, USA) containing equine IL-4 (eIL-4) [35], sequenced for correctness, and used to transiently transfect ExpiCHO-S cells, as per manufacturer's instructions (Thermo Fisher Scientific). The serum-free cell culture supernatant was harvested after 6 days of incubation and rIL-4/K42 fusion protein was purified using a HiTrap NHS-Activated HP affinity column coupled with aIL-4 monoclonal antibodies and an ÄKTA Fast Protein Liquid Chromatography (FPLC) instrument (GE Healthcare, Piscataway, NJ, USA). Immunizations, subsequent cell fusion, and mAb screening and selection were performed as previously described [35–37]. Briefly, one BALB/c mouse was immunized with 2 μg purified rIL-4/K42 fusion protein initially followed by 4 injections every 2–3 weeks

of 1 μg protein with an adjuvant (Adjuvant MM, Gerbu, Heidelberg, Germany). Three booster injections of 1 μg of rIL-4/K42 without adjuvant were performed prior to euthanasia. Mono-clonal antibodies (mAbs) were generated by fusion of splenic B cells from the immunized mouse and murine myeloma cells, as previously described [36].

K124 monoclonal antibodies. K124 mAbs were produced by Genscript (genscript.com, Piscataway, NJ, USA) by immunizing Balb/c mice with synthetic peptides targeting N-terminal and C-terminal regions of equine K124 (gene ID: 100061458) conjugated to keyhole limpet hemocyanin immunogen followed by splenic lymphocyte fusion with myeloma type SP2/0 cells. Three anti-K124 mAbs were evaluated in our laboratory, and are designated here as K124A (clone 9H8G1, murine isotype IgG2a), targeting the 14 amino acid peptide, (SVSQ GGKSFGGGFG) from positions 36–49 of the N-terminal region, and K124C (clone 4G6E9, murine isotype IgG1) and K124D (clone 4G7A3, murine isotype IgG2b), targeting (RIISK TSTKRSYRS), the last 14 amino acids (508–521) of the C-terminal region. Unpurified hybrid-oma supernatant was used for all K124 mAb experiments except for the immunoblot shown in S1 Fig, which was performed using protein A-purified K124A and K124C mAb generated by Genscript (genscript.com).

Immunoblot analysis

Total protein extraction and concentration determination were performed as previously described [23] from the following snap frozen tissues: hoof lamellar, haired skin, hoof coronet, corneal limbus, chestnut (an epidermal callus on the medial foreleg proximal to the carpus), tongue, oral mucosa, and preputial unhaired (glabrous) skin. SDS-PAGE and immunoblotting were performed as previously described [23], with 2–8 μg total protein loaded per lane and the following dilutions of mouse mAbs: anti-K14 (1:500; clone LL002, Abcam Inc., Cambridge, UK), anti-K42 (1:500), or anti-K124, clones K124A, K124C, or K124D (1:10) followed by sec-ondary goat-anti-mouse-horse radish peroxidase (HRP; 1:5,000, Jackson ImmunoResearch, Inc, West Grove, PA, USA). Chemiluminescence detection was performed by incubating blots for 1 min with 79 μM p-coumaric acid and 500 μM luminol mixed 1:1 with 3.6×10^{-3}% hydro-gen peroxide, both in 100 mM TRIS-HCl, pH 8.5 (all reagents: Sigma-Aldrich) followed by exposure to x-ray film (Hyperfilm™ ECL, GE Healthcare) for 1–3 min and x-ray film develop-ment. Immunoblots were reprobed with anti-keratin K14 and mouse anti-β-actin-HRP mAb (K124 blots; 1:15,000, clone AC-15; Sigma-Aldrich) or anti-β-actin-HRP alone (K42 blots) without stripping to demonstrate equal protein load. Following immunoblotting, proteins were visualized with Amido Black staining solution (Sigma-Aldrich) according to manufactur-er's directions.

Immunofluorescence

Indirect immunofluorescence using fluorescein-conjugated wheat germ agglutinin (F-WGA, Vector Laboratories, Burlingame, CA, USA) as a counterstain on paraformaldehyde-fixed/ sucrose-dehydrated/optimal cutting temperature compound (OCT)-embedded frozen tissue sections was performed as previously described, with the following modifications [32]. Anti-gens were unmasked through 20 min in Antigen Unmasking Solution (Vector Laboratories Inc.) in a 100°C steam bath, followed by cooling to RT on ice. Sections were next submerged for 15 min in 0.1 M glycine and 4 min on ice, followed by 20 min in Background Buster (Inno-vex Biosciences Inc., Richmond, CA, USA) at RT. Unpurified mouse anti-K124 mAb, clone K124C (1:10 dilution) served as primary antibody and goat anti-mouse Alexa Fluor™ 594 antibody (1:500 dilution; Invitrogen, Thermo Fisher Scientific) as the secondary antibody. Pri-mary and secondary antibody incubations were for 1 h at 23°C in a humidified chamber. All

antibodies were diluted in PBS containing 2% normal goat serum (Jackson ImmunoResearch). All wash steps following incubation with the primary antibody were performed in PBS/0.05% Tween-20.

Sections were mounted and imaged by confocal microscopy as previously described [32]. Primary antibody was omitted to determine background staining.

Results

KRT42 and *KRT124* mRNA is detected in hoof lamellae, but not haired skin, cornea, or hoof coronet

As shown in Fig 2, RT-PCR was performed to determine the qualitative tissue expression of K42 and K124, the major keratin isoforms that we had previously detected as proteins in equine hoof lamellar tissue, in the cornea, haired skin, hoof coronet and lamellar tissues. All RT-PCR products display molecular weights predicted to correspond to mRNA rather than genomic DNA (Fig 2, Table 1). The basal cell keratin, *KRT14*, was used as a positive control since it is expressed in all stratified epithelial tissues [38]. *KRT14* is expressed in cornea, haired skin, and lamellae, *KRT10A* and *KRT10B* expression is restricted to haired skin and of the two, *KRT10B* is more readily detected by this method. *KRT42* and *KRT124* mRNA is only detected in lamellar tissue and was not amplified from mRNA isolated from cornea, haired skin, or hoof coronet tissues.

KRT124 mRNA localizes to the hoof secondary epidermal lamellae and is absent from hoof coronet and haired skin

As shown in Figs 3 and 4, we employed in situ hybridization (ISH) to more precisely localize *KRT124* expression. *KRT124* was detected by ISH in all regions of the epidermal lamellae except for the central keratinized axis of the primary epidermal lamellae (Fig 3A). *KRT124* expression was not detected in the coronet or in haired skin (Fig 3B). Staining was also
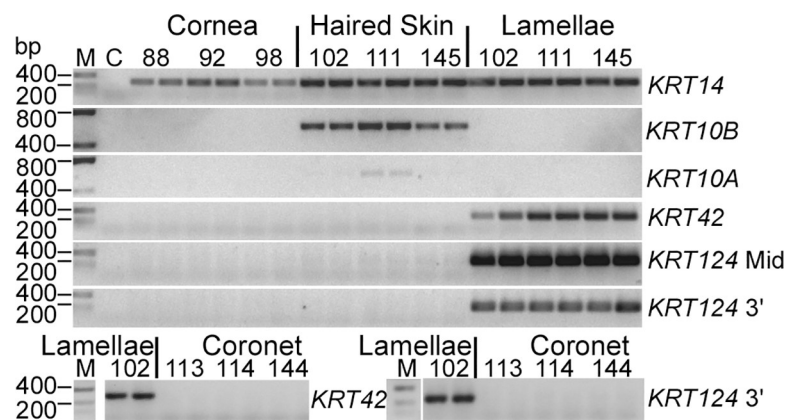
Fig 2. *KRT42* and *KRT124* are expressed in hoof lamellae, but not cornea, haired skin, and coronet. Representative RT-PCR products from equine cornea, haired skin, hoof lamellae, and hoof coronet, using primers for *KRT14*, *KRT10A*, *KRT10B*, *KRT42*, and *KRT124*, as indicated to the right of gels, and separated by agarose gel electrophoresis, produces amplicons of the expected base pair (bp) sizes, as indicated to the left of gels. RT-PCR products from duplicate experiments were run using RNA extracts from three different horses (identified by number above pairs of lanes) per tissue. DNA ladder (M), negative control without template RNA (C), and tissues identified above gels. Duplicate *KRT10* genes present in separate loci that were individually amplified using specific primers (*K10A* and *K10B*). Two sets of primers were used to amplify two different regions of *KRT124* (*KRT124* Mid and *KRT124* 3'). Image inverted for ease of viewing.
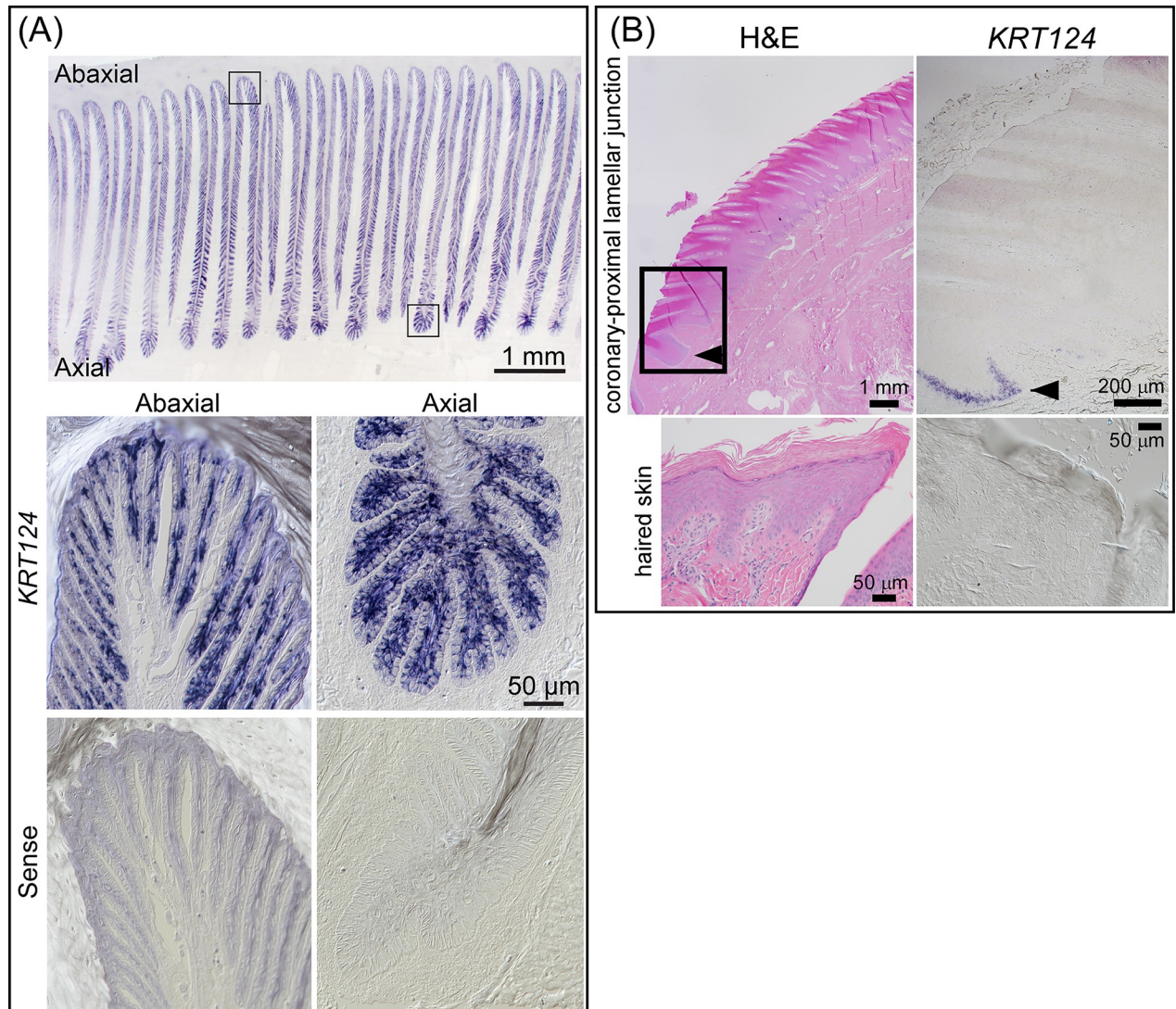
Fig 3. *KRT124* mRNA localizes to secondary epidermal lamellae and is absent from hoof coronet. (A) Representative images of *KRT124* localization to secondary epidermal lamellae (SELs) by in situ hybridization. *KRT124* localizes to suprabasal cells and, with less intense staining, to basal cells in all regions along the lamellae. Bottom panels: Representative differential interference contrast images of *KRT124* sense probe in situ hybridization shown as negative control. Axial (left) and abaxial (right) lamellar regions shown, corresponding to the axial and abaxial regions shown in top panel. Scale bar (50 μm) applies to all four lower panels. (**B**) Representative H&E and *KRT124* in situ hybridization images of a longitudinal section of the coronet and proximal lamella (arrowhead) and haired skin. Area of coronary-lamellar junction similar to the boxed area in the H&E image shows the abrupt transition from *KRT124*-negative keratinocytes in the coronary epithelium to *KRT124*-positive keratinocytes in a proximal lamella. All studies: n≥3 using samples from 9 horses, as detailed in S2 Table).

negative in lamellar tissue using a *KRT124* sense probe (Fig 3A, lower panels). An abrupt transition from *KRT124*-negative coronary epidermal tissue to *KRT124*-positive lamellar epidermal tissue is apparent at the junction between coronet and the first proximal lamella (Fig 3B).

Although *KRT124* ISH staining is apparent in both basal and suprabasal cells in some regions (Fig 3A), it was generally more intense in the suprabasal cells and lighter or absent from basal cells (Fig 4). *KRT14* ISH, in contrast, is restricted to basal cells in lamellar tissue (Fig 4), similar to the previously reported localization of K14 protein in healthy lamellar tissue [21;24;29]. The *KRT14* probe was designed to avoid cross-hybridization with the mRNA of other type I keratins. This short probe incorporates fewer DIG-labels and the color product is
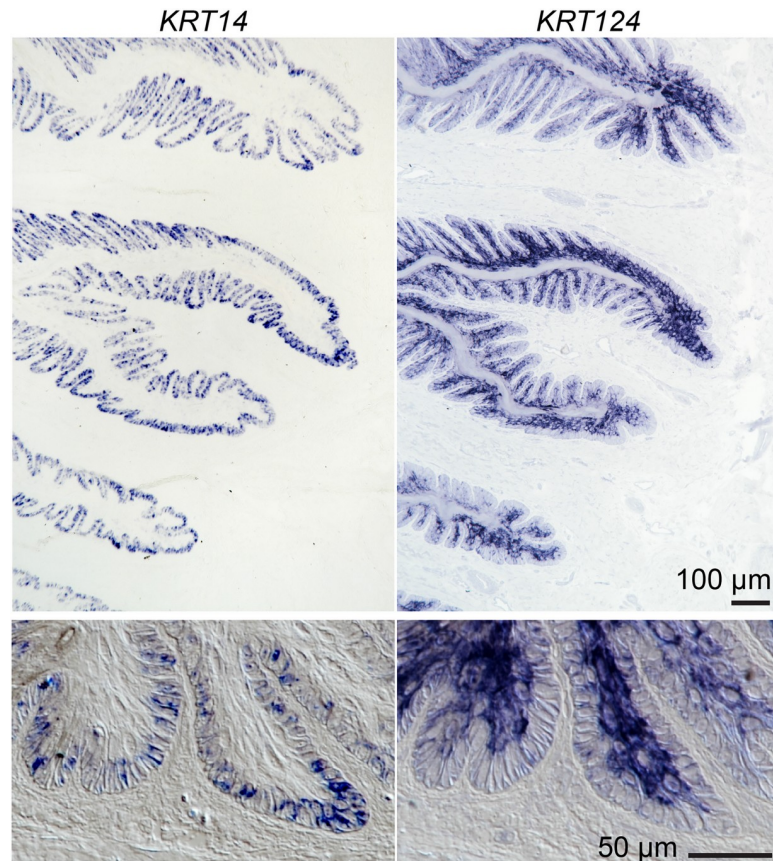
Fig 4. KRT14 and KRT124 mRNA localizes to basal and suprabasal cells of the secondary epidermal lamellae.
Representative images from in situ hybridization of *KRT14* (left) and *KRT124* (right) expression in serial sections.
KRT14 is restricted to basal cells, while *KRT124* is expressed primarily in suprabasal layers. Boxed regions marked on
low magnification images are shown below at higher magnification and include differential interference contrast
optics. All studies: n≥3 using samples from 9 horses, as detailed in S2 Table.

https://doi.org/10.1371/journal.pone.0219234.g004

therefore not detectable in every cell at higher magnification, but positive cells are confined to
the basal epidermal layer. Mature mRNA is mostly cytoplasmic and ISH color product is there-
fore deposited there and not within nuclei.

K42 and K124 monoclonal antibodies specifically detect hoof lamellar proteins on immunoblots

Monoclonal antibodies were generated against full-length recombinant equine K42 and
against two different peptides from K124, as described in the Methods section, and character-
ized by immunoblotting (Fig 5). As shown in Fig 5A, the anti-K42 mAb detects a single band
from lamellar tissue extract at the expected relative molecular mass (50 kDa), and co-migrates
with the second most abundant type 1 keratin in lamellar tissue, K14 [23]. Three anti-K124
mAb clones, K124A (against an N-terminal peptide), K124C, and K124D (the latter two
against a single C-terminal peptide) were immunoreactive for a single major band at the
expected relative molecular mass (54 kDa) in lamellar tissue extract (Fig 5A). The K14/K42
and K124 immunoblot bands correspond to two major protein bands that are visible by pro-
tein stain, even at the low total protein loads used for these studies (Fig 5A), as previously
reported [23]. Anti-K124 C-terminal peptide clones K124C and K124D also detected a lower

(A)

(B)
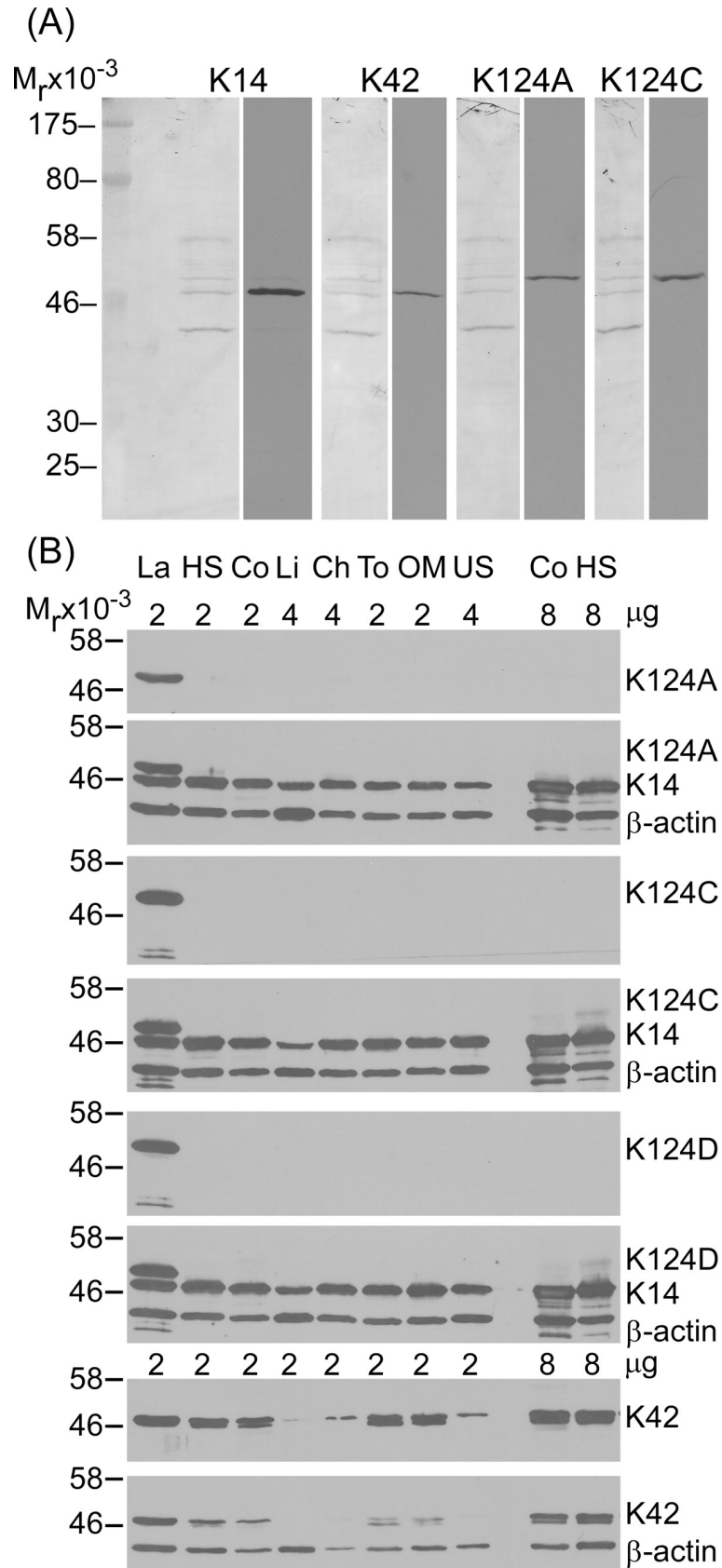
Fig 5. Detection of K14, K42, and K124 by immunoblotting with monoclonal antibodies. Representative immunoblots using mouse monoclonal anti-K14, anti-K42, or anti-K124 clones A, C, or D, as described in the Methods section (n≥3 per tissue using samples from 18 horses, as detailed in S2 Table). (A) Representative images of K14, K42, K124A, and K124C immunoblot strips (right images) and amido black stain for protein of each blot (left images) from the same SDS-PAGE gel with 2 μg lamellar protein loaded per lane. K14, K42, K124A and K124C immunoblots detect a single band at the expected relative molecular weight (M_r) in lamellar tissue. K14 and K42 co-localize to a 50 kDa band and the K124 mAbs are immunoreactive with a 54 kDa band. (B) K14, K42, and K124 immunoblots of epidermal and surface epithelial tissue extracts demonstrate the specificity of the K124 mAbs to lamellar tissue. La: lamellar; HS: haired skin; Co: coronary; Li: Corneal limbus; Ch: chestnut; To: tongue; OM: oral mucosa; US: unhaired (glabrous) skin. Total protein load per lane indicated above tissue labels. K124 and K42 immunoblots reprobed with K14 and β-actin (K124 blots) or β-actin alone (K42 blots) without stripping to demonstrate equal load. K42 mAb detects a single band in lamellar, chestnut, and unhaired skin tissues and a doublet band in haired skin, coronary, tongue, and oral mucosa tissues. All three K124 mAbs detect a single major band and, for K124C and K124D, an additional, lower relative molecular mass minor doublet band only in lamellar tissue. Increased protein load confirms negative K124 mAb cross-reactivity to keratins in coronet and haired skin (last two lanes).

relative molecular mass minor doublet band that is not visible by protein staining in some lamellar tissue samples under these immunoblotting conditions (Fig 5B).

Immunoblotting with multiple stratified epithelial tissues was performed to evaluate antibody cross-reactivity (Fig 5B). The anti-K42 mAb detects a single band in lamellar, chestnut, and unhaired skin tissues and a doublet band in haired skin, coronary, tongue, and oral mucosa tissues. Immunoreactivity to non-lamellar tissues is less apparent than immunoreactivity to lamellar tissue following additional washes, but still clearly present for haired skin, coronary, tongue, and oral mucosa, consistent with antibody cross-reactivity at this antibody concentration (lower blot, Fig 5B). All three anti-K124 mAbs show no cross-reactivity to any of the non-lamellar stratified epithelial tissues tested. Increased protein load confirmed negative anti-K124 mAb cross-reactivity to keratins in coronet and haired skin (last two lanes for each immunoblot). Immunoblots with protein A-purified anti-K124, clones A and C, detected a single 54 kDa band with an antibody dilution of 1:5,000 and as little as 25 ng total lamellar protein load (S1 Fig).

K124 monoclonal antibodies specifically localize to hoof epidermal lamellae

As shown in Fig 6, indirect immunofluorescence using the anti-K124C mAb on cryosections demonstrates localization of K124 to the epidermal lamellae in a pattern that resembles that obtained by KRT124 ISH (Figs 3 and 4). K124 localizes to suprabasal cells, and to a lesser degree, basal cells of all secondary epidermal lamellae. The keratinized axes of the primary epidermal lamellae are negative. Anti-K124C did not show any specific immunoreactivity to coronet or haired skin. Negative control experiments that omitted the primary K124C antibody were run in parallel on serial lamellar tissue cryosections. The negative controls showed minimal non-specific staining or autofluorescence of red blood cells in lamellar tissue, similar to that observed for the coronary and haired skin images shown in Fig 6, but no lamellar tissue-specific immunoreactivity (S2 Fig).

Discussion

To our knowledge, this is the first report of the use of isoform-specific antibodies to localize a nail unit-specific keratin isoform (K124) in any species. In addition, this is the first demonstration that the expression of K124 is restricted to the equine (E. caballus) hoof lamellae, the highly folded inner epithelium of the hoof capsule, which is homologous to the nail bed of primates, rodents, and other species, and is absent from the germinative ("coronary") region of
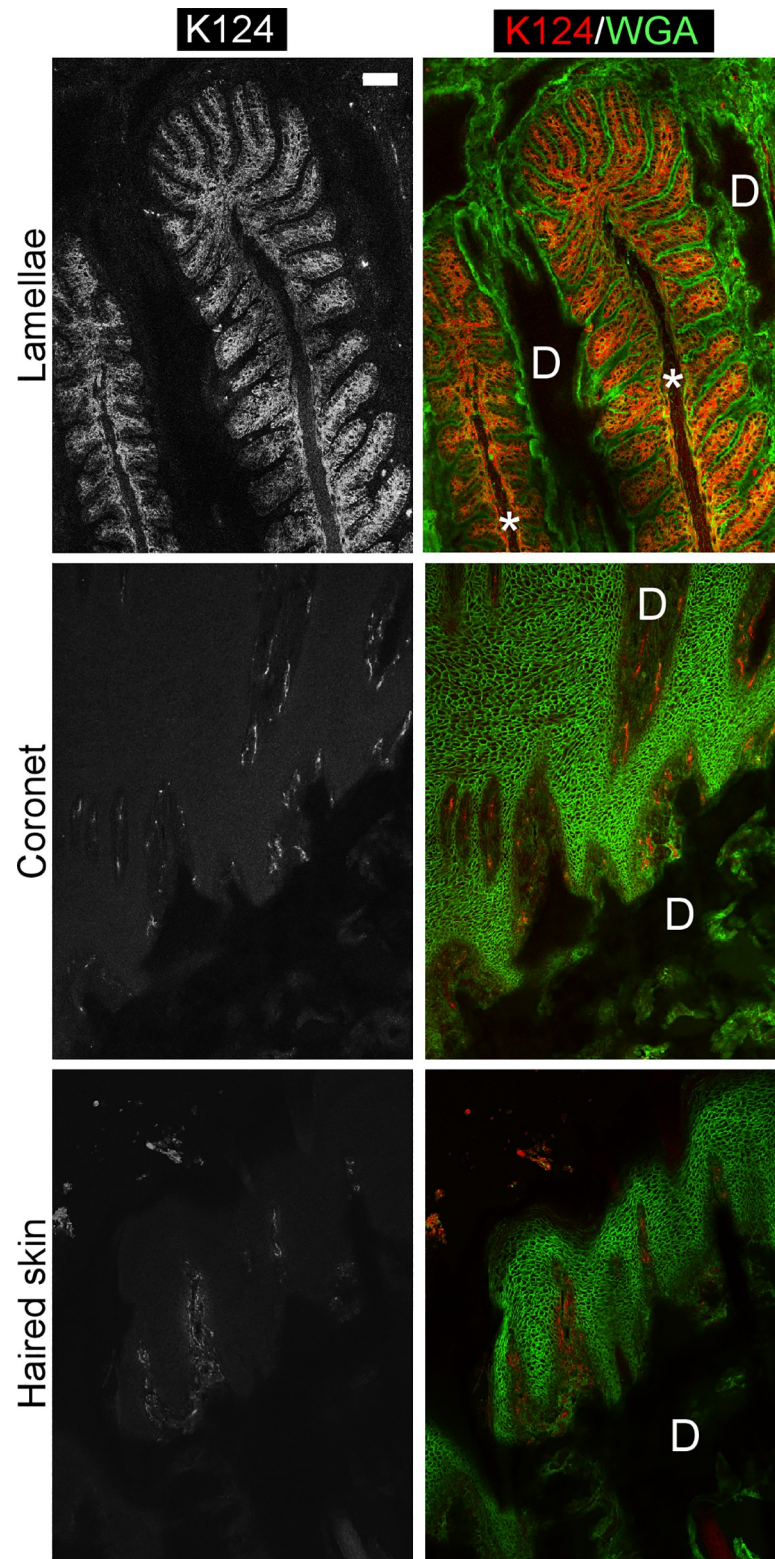
Fig 6. Localization of K124 to basal and suprabasal secondary epidermal lamellar cells by indirect immunofluorescence. Cryosections from lamellar, coronet, and haired skin frozen tissues were subjected to indirect immunofluorescence using the K124C mAb and fluorescein-conjugated wheat germ agglutinin (WGA) as a counterstain, as described in the Methods section (n = 3–4 using samples from 7 horses, as detailed in S2 Table). The

left panels show the red channel (K124) in monochromatic grayscale and the right panels show the merged red (K124) and green (WGA) pseudocolor images. K124C localizes to suprabasal cells, and to a lesser degree, basal cells of all SELs. Coronet and haired skin show negative staining for K124, with some autofluorescence of red blood cells visible in dermal tissues. (D): dermis; *: Keratinized axis of PEL. Scale bar = 20 μm. Images were collected and adjusted under identical settings.

the proximal hoof wall, which is homologous to the nail matrix [26;39;40]. K124 is the most abundant type II keratin of lamellar tissue [23] and, shown here (Figs 3, 4 and 6), its expression is increased in suprabasal, compared to basal, lamellar keratinocytes, suggesting it is a terminal differentiation marker for these cells. In contrast, the absence of K124 mRNA and protein in the coronary region indicates that this keratin isoform does not contribute to the hoof wall.

KRT124 and *KRT42* were recently identified by total RNA sequencing from canine and equine skin, suggesting that transcripts for these keratins are found in equine haired skin, although this result was not validated by any complementary methods [25]. We amplified neither *KRT124* nor *KRT42* from haired skin total RNA by RT-PCR (Fig 2), nor did we localize K124 to haired skin by ISH, immunoblotting, or indirect immunofluorescence histology (Figs 3 and 6), using samples from multiple horses of several breeds (S1 and S2 Tables). It is possible that the discrepancy relates either to the sensitivity of RNA-seq relative to our RT-PCR assay for the detection of very low abundance mRNA transcripts or to the anatomic location of the skin samples used since we collected samples from the dorsal region of the digit and the location of the skin biopsy used by Balmer, et al., is not specified [25]. Further investigation of equine skin keratin isoform expression is required to resolve this issue.

The rodent ortholog of *KRT124*, *Krt90* (formerly *Kb15*) and the opossum ortholog (*Kb15*) have not been characterized beyond genomic mapping and identification as likely functional genes in those species [27;28]. However, based on the relative protein amounts of K42 and K124 in lamellar tissue, we had previously suggested that these keratins hybridize in lamellar tissue, and are therefore expected to co-localize in the hoof lamellae [23]. Murine *Krt42* (formerly *K17n*) expression has been localized to the nail matrix and nail bed and functional canine *KRT42* and *KRT124* genes have been identified, suggesting that the nail bed expression of K42 and K124/K90 may be conserved across mammalian and marsupial species, but was lost from the thinner and non-weight-bearing nail units of primates, where both keratins exist only as pseudogenes [25–27]. Equine *KRT42* and *KRT124* have a more restricted tissue localization than murine *Krt42*. Murine *Krt42* is expressed in the nail matrix [27], but the equine lamellar-restricted keratins are not expressed in the homologous coronary region of the hoof wall, as assessed by RT-PCR for *KRT42* (Fig 2) and multiple methods for *KRT124*/K124 (Figs 2–6). The isoform-specific anti-K124 mAbs described here may allow protein localization and tissue distribution of K124/K90 in other species, possibly including studies of murine models of nail disease [41] and comparative evolutionary-developmental biology [25;42].

The tissue-restricted expression of keratin isoforms is of interest with regard to the mechanical function of the equine hoof capsule. Mouse keratin knock-out studies have demonstrated the crucial role of keratins in the maintenance of epithelial and cellular integrity in response to mechanical stress [3]. Knockout of all keratin genes significantly softens cells, reduces cell viscosity, and elevates plastic cell deformation on force application. Re-expression of a single keratin gene pair restores those mechanical properties [3]. The mechanical properties of keratin function in weight-bearing and dissipation of force in the cornified hoof capsule. In particular, the weight-bearing hoof wall is comprised of pressure-resistant hard-keratinized tubular horn whereas the lamellae, which constitute the epidermal component of the SADP, are comprised of softer, tensile-resistant keratinized tissue [14]. As we and others have shown, these hoof capsule regions differ in keratin isoform composition [21;43]. Keratins comprise approximately

80% of the total protein content in differentiated cells of stratified epithelia [2] and K42 and K124 constitute approximately 50% of the keratin content of lamellar tissue [23]. These keratins are therefore the most abundant and probably the most significant determinants of epidermal lamellar resistance to mechanical stress. Moreover, equine *KRT124* has a unique 3' region exon, as shown by the specificity of our RT-PCR primers for that region. This 3' exon encodes the tail region, including the peptide detected by the K124C and K124D mAbs. The tail region of K124 may be important in the specific self-assembly, bundling, interactions with keratin filament-associated proteins and adhesion complexes, and specific mechanical properties of K124-containing keratin filaments [2;11]. Further study is needed to determine how the molecular structure of K42 and K124 specifically contribute to the mechanical properties of the lamellae.

As proteins that contribute to the mechanical properties of the epidermis and epidermal appendages, keratin diversification contributes to the evolution of these structures and the ability of animals to exploit new ecological niches. The keratin gene family has undergone paralogous expansion in horses in comparison to dogs [25], humans, and cows [44], perhaps reflecting the importance of the hoof as a key evolutionary adaptation in this species. The expansion of the β-keratin gene family in birds is thought to have been important for the evolution of the morphological and structural diversity of avian skin appendages, including feather compositional adaptations needed for different lifestyles [45;46]. Conversely, Ehrlich, et al. recently reported that certain aquatic mammals, including cetaceans and manatees, have undergone a contraction of the keratin gene family, perhaps associated with the loss of epidermal appendages such as hairs and claws [42]. These animals have undergone replacement of the primary keratin pair of suprabasal keratinocytes in terrestrial mammalian skin, K1 and K10, with K6 and K17, a keratin pair normally expressed in response to epidermal stress and associated with epidermal thickening, underscoring the importance of keratin isoform expression to epidermal specialization. The morphogenesis of the equine hoof, as the most complex mammalian integumentary structure [14], is likewise dependent upon temporal and spatial expression of specific keratin isoforms for its development and mechanical function. Viewed together with our findings, these studies highlight the importance of keratin isoform expression in integumentary system adaptations that impact physiology, locomotion, the ability of animals to exploit new environments, and their use by humans as domesticated animals.

The biology of equine lamellae is also of interest due to the prevalence of equine laminitis, a common and devastating disease affecting this tissue. Laminitis results in epidermal pathologies that include abnormal hyperplastic and acanthotic epidermal tissue [19], epidermal dysplasia and metaplasia, loss of cell adhesion, apoptosis, and necrosis [20], and expression of cellular stress, activation, and altered differentiation markers [29;47–49]. Similar nail abnormalities involving the nail bed were recently described in association with ageing in several inbred strains of mice [41]. Our anti-K124 mAbs will be useful for the investigation of histopathological changes in lamellar and nail bed keratin expression and as a tissue-specific differentiation marker for *in vitro* studies. Moreover, changes in lamellar epidermal morphology and increases in apoptotic and necrotic cell counts associated with laminitis are consistent with a loss of keratin cytoskeletal architecture and may indicate degradation of keratin intermediate filaments [48;50;51]. Degraded keratins in other stressed or dying epithelial cells form cytoplasmic inclusion bodies, are found in cell surface blebs, and can circulate in blood as extracellular vesicles, apoptotic bodies, or free protein [52]. Keratins, as the most abundant proteins and as epithelial-specific proteins, are useful biomarkers of epithelial cell stress, apoptosis and necrosis in several human diseases, including various carcinomas [53] and several types of liver disease [52]. K124 could similarly serve as a tissue-specific disease biomarker for equine laminitis and nail unit disease in other species that express it.

In conclusion, we have characterized the expression of keratin isoforms that specifically localize to the highly specialized inner epithelium of the equine hoof capsule. For the first time, we have generated and characterized nail unit-specific anti-K124 mAbs, which localize specifically to the epidermal lamellae of the inner hoof capsule and do not cross-react with proteins from several stratified epithelial tissues. We propose that these hoof-specific keratins are essential components of the equine SADP and contribute to the mechanical properties of strength and elasticity of the inner hoof capsule that are necessary for single digit, unguligrade locomotion in the equidae, a signature evolutionary adaptation of this genus.

Supporting information

S1 Fig. Detection of K124 by immunoblotting with low protein load and affinity-purified monoclonal antibodies. Representative immunoblots using affinity-purified anti-K124 mAb, clones A (left) and C (right) at 1:5,000 dilution. Total protein extracted from lamellar tissue from three horses (two shown, as indicated above blots) loaded at 50 ng and 25 ng per lane (as indicated above blots). K124 and β-actin immunoblotting and detection were performed as described in the Methods section with the exception that chemiluminescence detection was performed using 2.5 mM luminol and 390 μM p-coumaric acid (5x strength). K124A and K124C are immunoreactive with a 54 kDa relative molecular mass (M_r) band, which is clearly visible at 50 ng and 25 ng total protein load for K124C and 50 ng protein load for K124A.
(TIF)

S2 Fig. Indirect immunofluorescence negative control for lamellar tissue. Lamellar tissue cryosection, serial to the one shown in Fig 6, subjected to indirect immunofluorescence and fluorescein-conjugated wheat germ agglutinin (WGA) as a counterstain, omitting the K124C mAb to show non-specific staining (n = 3 using samples from 3 horses, representative image shown). (A) Red channel, secondary antibody alone (white). (B) Secondary antibody alone (red) and fluorescein-WGA counterstain (green). Scale bar = 20 μm. Images were collected and adjusted under settings identical to those applied to Fig 6.
(TIF)

S1 Table. Breed, age, and sex of horses (*E. caballus*) used in experiments.
(PDF)

S2 Table. Horses (*E. caballus*) used for each experiment.
(PDF)

S1 File. Sanger sequencing validation for keratin isoform RT-PCR products. DNA chromatogram files of all of the keratin isoform RT-PCR products. The forward and reverse reads (designated "F" and "R" in the file names, respectively) were generated using the appropriate primer from Table 1. Alignment to expected sequences listed in Table 1 was confirmed by BLAST (blast.ncbi.nlm.nih.gov).
(ZIP)

S2 File. Sequence validation for gene synthesis and cloning of *KRT14* used for in situ hybridization. Sequence of the multicloning site of pBlueScript SK(+) plasmid after insertion of the *KRT14* sequence bp 1371–1667 into 5' NotI and 3'KpnI sites. See NM_001346198 for the entire mRNA sequence of *KRT14*. M13 forward and reverse primer binding sites that flank the vector multicloning site were used for sequencing.
(AB1)

S3 File. Sequence validation for gene synthesis and cloning of *KRT124* used for in situ hybridization. Sequence of the multicloning site of pBlueScript SK(+) plasmid after insertion of the *KRT124* sequence bp 1623–2307 into 5' NotI and 3'XhoI restriction sites. See XM_001504397.3 for the entire mRNA sequence of *KRT124*. M13 forward and reverse primer binding sites that flank the vector multicloning site were used for sequencing. (AB1)

Acknowledgments

Author Contributions

Conceptualization: Hannah Galantino-Homer.

Funding acquisition: Lynne Cassimeris, Bettina Wagner, Hannah Galantino-Homer.

Investigation: Caitlin Armstrong, Lynne Cassimeris, Claire Da Silva Santos, Yagmur Micoogullari, Susanna Babasyan, Hannah Galantino-Homer.

Methodology: Bettina Wagner, Samantha Brooks.

Supervision: Lynne Cassimeris, Bettina Wagner, Hannah Galantino-Homer.

Visualization: Lynne Cassimeris, Hannah Galantino-Homer.

Writing – original draft: Caitlin Armstrong, Lynne Cassimeris, Hannah Galantino-Homer.

Writing – review & editing: Claire Da Silva Santos, Yagmur Micoogullari, Susanna Babasyan, Samantha Brooks.

References

1. Schweizer J, Bowden PE, Coulombe PA, Langbein L, Lane EB, Magin TM, et al. New consensus nomenclature for mammalian keratins. J Cell Biol 2006; 174:169–74. https://doi.org/10.1083/jcb.200603161 PMID: 16831889

2. Bragulla HH, Homberger DG. Structure and functions of keratin proteins in simple, stratified, keratinized and cornified epithelia. J Anatomy 2009; 214:516–59.

3. Ramms L, Fabris G, Windoffer R, Schwarz N, Springer R, Zhou C, et al. Keratins as the main component for the mechanical integrity of keratinocytes. Proc Natl Acad Sci U S A 2013; 110(46):18513–8. https://doi.org/10.1073/pnas.1313491110 PMID: 24167246

4. Homberg M, Magin TM. Beyond expectations: novel insights into epidermal keratin function and regulation. Int Rev Cell Mol Biol 2014; 311:265–306. https://doi.org/10.1016/B978-0-12-800179-0.00007-6 PMID: 24952920

5. Lane EB, McLean WH. Keratins and skin disorders. J Pathol 2004; 204(4):355–66. https://doi.org/10.1002/path.1643 PMID: 15495218

6. Liao H, Sayers JM, Wilson NJ, Irvine AD, Mellerio JE, Baselga E, et al. A spectrum of mutations in keratins K6a, K16 and K17 causing pachyonychia congenita. J Derm Sci 2007; 48:199–205.

7. McGowan KM, Coulombe PA. Keratin 17 expression in the hard epithelial context of the hair and nail, and its relevance for the pachyonychia congenita phenotype. J Invest Dermatol 2000; 114(6):1101–7. https://doi.org/10.1046/j.1523-1747.2000.00986.x PMID: 10844551

8. Jin L, Wang G. Keratin 17: a critical player in the pathogenesis of psoriasis. Med Res Rev 2014; 34 (2):438–54. https://doi.org/10.1002/med.21291 PMID: 23722817

9. Fuchs E, Weber K. Intermediate filaments: Structure, dynamics, function, and disease. Annu Rev Biochem 1994; 63:345–82. https://doi.org/10.1146/annurev.bi.63.070194.002021 PMID: 7979242

10. Moll R, Divo M, Langbein L. The human keratins: biology and pathology. Histochem Cell Biol 2008; 129:705–33. https://doi.org/10.1007/s00418-008-0435-6 PMID: 18461349

11. Lee CH, Coulombe PA. Self-organization of keratin intermediate filaments into cross-linked networks. J Cell Biol 2009; 186(3):409–21. https://doi.org/10.1083/jcb.200810196 PMID: 19651890

12. Davies HMS, Merritt JS, Thomason JJ. Biomechanics of the equine foot. In: Floyd AE, Mansmann RA, editors. Equine Podiatry. St. Louis, MO: Saunders Elsevier; 2007. p. 42–56.

13. Roland ES, Hull ML, Stover SM. Design and demonstration of a dynamometric horseshoe for measuring ground reaction loads of horses during racing conditions. J Biomech 2005; 38(10):2102–12. https://doi.org/10.1016/j.jbiomech.2004.08.024 PMID: 16084211

14. Bragulla H, Hirschberg RM. Horse hooves and bird feathers: Two model systems for studying the structure and development of highly adapted integumentary accessory organs—The role of the dermo-epidermal interface for the micro-architecture of complex epidermal structures. J Exp Zool 2003; 298B:140–51.

15. Pollitt CC. The anatomy and physiology of the suspensory apparatus of the distal phalanx. Vet Clin North Am Equine Pract 2010; 26:29–49. https://doi.org/10.1016/j.cveq.2010.01.005 PMID: 20381734

16. MacFadden BJ. What's the use? Functional morphology of feeding and locomotion. Fossil horses: Systematics, paleobiology, and evolution of the family equidae. New York, NY: Cambridge University Press; 1992. p. 229–62.

17. Fleckman P, Jaeger K, Silva KA, Sundberg JP. Comparative anatomy of mouse and human nail units. Anat Rec (Hoboken) 2013; 296(3):521–32.

18. Hood DM. The mechanisms and consequences of structural failure of the foot. Vet Clin North Am Equine Pract 1999; 15(2):437–61. PMID: 10472121

19. Collins SN, Van Eps AW, Kuwano A, Pollitt CC. The Lamellar Wedge. Vet Clin North Am Equine Pract 2010; 26:179–95. https://doi.org/10.1016/j.cveq.2010.01.004 PMID: 20381746

20. Engiles JB, Galantino-Homer H, Boston R, McDonald D, Dishowitz M, Hankenson KD. Osteopathology in the equine distal phalanx associated with the development and progression of laminitis. J Vet Pathol 2015; 52(5):928–44.

21. Wattle O. Cytokeratins of the equine hoof wall, chestnut and skin: bio- and immunohisto-chemistry. Equine Vet J Suppl 1998; 26:66–80.

22. Wattle O. Cytokeratins of the stratum medium and stratum internum of the equine hoof wall in acute laminitis. Acta Vet Scand 2000; 41(4):363–79. PMID: 11234970

23. Carter RA, Shekk V, de Laat MA, Pollitt CC, Galantino-Homer HL. Novel keratins identified by quantitative proteomic analysis as the major cytoskeletal proteins of equine (Equus caballus) hoof lamellar tissue. J Anim Sci 2010 Jul 9; 88(12):3843–55. https://doi.org/10.2527/jas.2010-2964 PMID: 20622188

24. Linardi R, Megee S, Mainardi S, Senoo M, Galantino-Homer H. Expression and localization of epithelial stem cell and differentiation markers in equine skin, eye and hoof. Vet Dermatol 2015; 26(4):213–e47. https://doi.org/10.1111/vde.12214 PMID: 25963063

25. Balmer P, Bauer A, Pujar S, McGarvey KM, Welle M, Galichet A, et al. A curated catalog of canine and equine keratin genes. PLoS One 2017; 12(8):e0180359. https://doi.org/10.1371/journal.pone.0180359 PMID: 28846680

26. Tong X, Coulombe PA. A novel mouse type I intermediate filament gene, keratin 17n (K17n), exhibits preferred expression in nail tissue. J Invest Dermatol 2004; 122:965–70. https://doi.org/10.1111/j.0022-202X.2004.22422.x PMID: 15102087

27. Hesse M, Zimek A, Weber K, Magin TM. Comprehensive analysis of keratin gene clusters in humans and rodents. European Journal of Cell Biology 2004; 83:19–26. https://doi.org/10.1078/0171-9335-00354 PMID: 15085952

28. Zimek A, Weber K. The organization of the keratin I and II gene clusters in placental mammals and marsupials show a striking similarity. European Journal of Cell Biology 2006; 85:83–9. https://doi.org/10.1016/j.ejcb.2005.10.001 PMID: 16439307

29. Carter RA, Engiles JB, Megee SO, Senoo M, Galantino-Homer HL. Decreased expression of p63, a regulator of epidermal stem cells, in the chronic laminitic equine hoof. Equine Veterinary Journal 2011; 43(5):543–51. https://doi.org/10.1111/j.2042-3306.2010.00325.x PMID: 21496086

30. Galantino-Homer H, Carter R, Megee S, Engiles J, Orsini J, Pollitt C. The Laminitis Discovery Database. J Equine Vet Sci 2010; 30(2):101.

31. Pollitt CC. Basement membrane pathology: a feature of acute equine laminitis. Equine Veterinary Journal 1996; 28(1):38–46. https://doi.org/10.1111/j.2042-3306.1996.tb01588.x PMID: 8565952

32. Clark RK, Galantino-Homer H. Wheat Germ Agglutinin as a Counterstain for Immunofluorescence Studies of Equine Hoof Lamellae. Exp Dermatol 2014; 23(9):677–8. https://doi.org/10.1111/exd.12495 PMID: 25040657

33. Untergasser A, Cutcutache I, Koressaar T, Ye J, Faircloth BC, Remm M, et al. Primer3—new capabilities and interfaces. Nucleic Acids Research 2012; 40(15):e115. https://doi.org/10.1093/nar/gks596 PMID: 22730293

34. Wolenski FS, Layden MJ, Martindale MQ, Gilmore TD, Finnerty JR. Characterizing the spatiotemporal expression of RNAs and proteins in the starlet sea anemone Nematostella vectensis. Nat Protoc 2013; 8:900–15. https://doi.org/10.1038/nprot.2013.014 PMID: 23579779

35. Wagner B, Hillegas JM, Babasyan S. Monoclonal antibodies to equine CD23 identify the low-affinity receptor for IgE on subpopulations of IgM+ and IgG1+ B-cells in horses. Vet Immunol Immunopathol 2012; 146(2):125–34. https://doi.org/10.1016/j.vetimm.2012.02.007 PMID: 22405681

36. Wagner B, Radbruch A, Rohwer J, Leibold W. Monoclonal anti-equine IgE antibodies with specificity for different epitopes on the immunoglobulin heavy chain of native IgE. Vet Immunol Immunopathol 2003; 92(1–2):45–60. https://doi.org/10.1016/s0165-2427(03)00007-2 PMID: 12628763

37. Schnabel CL, Wemette M, Babasyan S, Freer H, Baldwin C, Wagner B. C-C motif chemokine ligand (CCL) production in equine peripheral blood mononuclear cells identified by newly generated monoclonal antibodies. Vet Immunol Immunopathol 2018; 204:28–39. https://doi.org/10.1016/j.vetimm.2018.09.003 PMID: 30596378

38. Porter RM, Lunny DP, Ogden PH, Morley SM, McLean WH, Evans A, et al. K15 expression implies lateral differentiation within stratified epithelial basal cells. Lab Invest 2000; 80(11):1701–10. PMID: 11092530

39. De Berker D, Wojnarowska F, Sviland L, Westgate GE, Dawber RPR, Leigh IM. Keratin expression in the normal nail unit: Markers of regional differentiation. Brit J Dermatol 2000; 142:89–96.

40. Daradka M, Pollitt CC. Epidermal cell proliferation in the equine hoof wall. Equine Veterinary Journal 2004; 36:236–41. https://doi.org/10.2746/0425164044877198 PMID: 15147131

41. Linn SC, Mustonen AM, Silva KA, Kennedy VE, Sundberg BA, Bechtold LS, et al. Nail abnormalities identified in an ageing study of 30 inbred mouse strains. Exp Dermatol 2019; 28:383–90. https://doi.org/10.1111/exd.13759 PMID: 30074290

42. Ehrlich F, Fischer H, Langbein L, Praetzel-Wunder S, Ebner B, Figlak K, et al. Differential evolution of the epidermal keratin cytoskeleton in terrestrial and aquatic mammals. Mol Biol Evol 2018.

43. Grosenbaugh DA, Hood DM. Keratin and associated proteins of the equine hoof wall. Am J Vet Res 1992; 53(10):1859–63. PMID: 1280927

44. Wade CM, Giulotto E, Sigurdsson S, Zoli M, Gnerre S, Imsland F, et al. Genome sequence, comparative analysis, and population genetics of the domestic horse. Science 2009; 326:865–7. https://doi.org/10.1126/science.1178158 PMID: 19892987

45. Zhang G, Li C, Li Q, Li B, Larkin DM, Lee C, et al. Comparative genomics reveals insights into avian genome evolution and adaptation. Science 2014; 346(6215):1311–20. https://doi.org/10.1126/science.1251385 PMID: 25504712

46. Wu P, Ng CS, Yan J, Lai Y-C, Chen C-K, Lai Y-T, et al. Topographical mapping of α- and β-keratins on developing chicken skin integuments: Functional interaction and evolutionary perspectives. Proc Natl Acad Sci U S A 2015;E6770–E6779. https://doi.org/10.1073/pnas.1520566112 PMID: 26598683

47. Leise BS, Watts M, Roy S, Yilmaz S, Alder H, Belknap JK. Use of laser capture microdissection for the assessment of equine lamellar basal epithelial cell signalling in the early stages of laminitis. Equine Vet J 2015; 47(4):478–88. https://doi.org/10.1111/evj.12283 PMID: 24750316

48. Cassimeris L, Engiles JB, Galantino-Homer H. Detection of endoplasmic reticulum stress and the unfolded protein response in naturally-occurring endocrinopathic equine laminitis. BMC Vet Res 2019; 15(1):24. https://doi.org/10.1186/s12917-018-1748-x PMID: 30630474

49. Faleiros RR, Nuovo GJ, Belknap JK. Calprotectin in myeloid and epithelial cells of laminae from horses with black walnut extract-induced laminitis. J Vet Intern Med 2009; 23(1):174–81. https://doi.org/10.1111/j.1939-1676.2008.0241.x PMID: 19175737

50. Strnad P, Paschke S, Jang KH, Ku NO. Keratins: markers and modulators of liver disease. Curr Opin Gastroenterol 2012; 28(3):209–16. https://doi.org/10.1097/MOG.0b013e3283525cb8 PMID: 22450891

51. Karikoski NP, McGowan CM, Singer ER, Asplin KE, Tulamo R-M, Patterson-Kane JC. Pathology of natural cases of equine endocrinopathic laminitis associated with hyperinsulinemia. Vet Pathol 2014;Epub 17 Sep. pii: 0300985814549212.

52. Ku NO, Strnad P, Bantel H, Omary MB. Keratins: Biomarkers and modulators of apoptotic and necrotic cell death in the liver. Hepatology 2016; 64(3):966–76. https://doi.org/10.1002/hep.28493 PMID: 26853542

53. Linder S, Olofsson MH, Herrmann R, Ulukaya E. Utilization of cytokeratin-based biomarkers for pharmacodynamic studies. Expert Rev Mol Diagn 2010; 10(3):353–9. https://doi.org/10.1586/erm.10.14 PMID: 20370591